Journal of Research and Applications in Mechanical Engineering
ISSN: 2229-2152 (Print); 2697-424x (Online)
(2024) Vol. 12, No. 1, Paper No. JRAME-24-12-002
[DOI: 10.14456/jrame.2024.2]

Research Article

Analysis and Design for Vibration of a Wing-Like Laminated Composite Panel with Blended Layers

Y. Narita*
Faculty of Engineering (Professor Emeritus), Hokkaido University, Sapporo, Japan

Received 21 January 2023
Revised 2 May 2023
Accepted 9 June 2023

Abstract:
An analytical method is presented to study the bending vibration of a cantilevered, laminated composite rectangular panel having blended layers. The panel (plate) having blended layers is modelled as a laminated plate in which the outer layers have subdivisions with non-identical fiber orientation. A finite element program is also coded to clarify accuracy of the present method. In numerical examples, the natural frequencies computed by the proposed method show very good agreement with those from the FEM code. Use of this fast and accurate method is suggested in vibration design, for example, optimization of fundamental frequencies.

Keywords: *Laminates, Blended layer, Natural frequency, Energy method, FEM*

1. Introduction

Advanced laminated composites have been applied in the past few decades to actual structures, and academic and technical demands became obvious for more details on dynamic nature of cantilevered composite plates. Some textbooks on mechanics of composite plates were issued by various authors [1-3]. A textbook with considerable weight on composites for aircraft applications was published [4]. Innovative use of advanced composites is introduced in the airplane structures [5] and morphing function [6].

Among various types of composite plates, the free vibration of cantilever plates (flat panels) has been extensively studied, because a cantilever plate is used as an analytical model for airplane wings, turbine blades and other structural applications. A well-known monograph was released in 1969 (reprinted version in 1993) by Leissa [7] to cover the plate vibration, and rigorous lists of natural frequencies were presented for cantilever plates [8, 9]. In particular, reference [8] is a comprehensive summary of many previous investigations on the free vibration of cantilever plates which are results of a joint industry, government and university effort.

A composite laminate is taken into account here to have layer (lamina) composed of parallel fibers embedded in a matrix material. The fiber and matrix material are carbon fiber and epoxy resin, respectively, in this study. Each layer has material orthotropy caused from high stiffness of fibers, that is, non-identical elastic constants in the fiber direction and the transverse direction in the plane. Although such dependence on direction causes complication in mechanics, tailoring of the laminate can be made by intentionally stacking layers. Introduction of optimization is one of such recent technical trends in the vibration design, and for reference, Ghiasi and his colleagues [10, 11] outlined progress of various optimum design up to the year of 2010. Recently, it becomes possible to fabricate composites reinforced by continuously curved fibers. Since the fibers have variable anisotropy in the same layer, it is feasible

* Corresponding author: Y. Narita
E-mail address: ynarita@eng.hokudai.ac.jp

to design in the range of larger degree-of-freedom. In other words, the laminated composite with optimally deployed curvilinear fibers may exhibit significant mechanical improvements, and some references are obtained for such problems [12-20]. These papers demonstrate possibility of more effective design, but the high cost of manufacturing such composite plates is still serious problem. Alternative solution to it is the use of blended layers [9, 21-23] or alike ideas to refrain from high cost of distributing curvilinear fibers and design complexity in optimum design. The plate with blended layer is a laminated plate possessing (outer) layers of multiple subdivisions with non-identical orientation angles of straight fibers.

In the present paper, a practical approach is given to analyze bending vibration of cantilevered, laminated composite plates with blended layers, and numerical results are obtained in good accuracy for the problem. The blended plate here is defined to have some layers made of two or more subdivisions with different fiber orientations. The Ritz method is used as a basic approach to include non-identical bending stiffness in the subdivisions. The energy functional is evaluated by integrating over all subdivisions. By utilizing the same classical plate theory, the finite element method (FEM) code is also developed [23] to assess accuracy of the Ritz results. General-purpose commercial FEM programs were not used to evade ambiguity as a black box. Furthermore, design aspect is discussed for the present extension. In the design of small number of design variables, permutation approach is practical by making use of short computing time of the present method. One of metaheuristic approaches, such as GA (genetic algorithm) or PSO (particle swarm optimization) may be employed in larger size problem to obtain approximate optimum solutions.

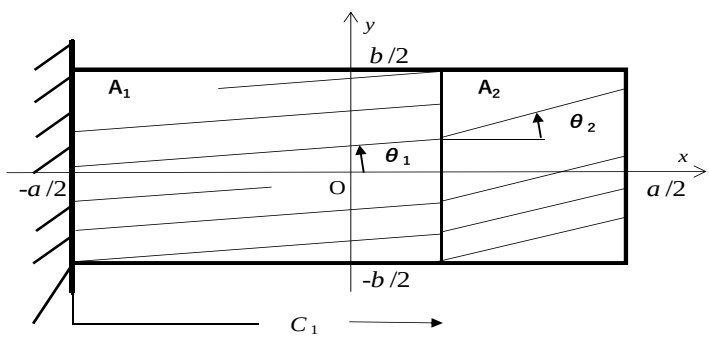

Fig. 1. Cantilevered, laminated composite rectangular plate with two subdivisions: Area 1 (A_1) and Area 2 (A_2).

2. Vibration analysis

Figure 1 presents a symmetrically laminated plate to have two subdivisions. Each subdivision possesses straight fibers uniformly distributed with prescribed orientation angle. The stress-strain relation in *p*-th subdivision is given in the *k*-th layer by

$$\begin{Bmatrix} \sigma_x \\ \sigma_y \\ \tau_{xy} \end{Bmatrix}^{(k,p)} = \begin{bmatrix} \bar{Q}_{11} & \bar{Q}_{12} & \bar{Q}_{16} \\ \bar{Q}_{12} & \bar{Q}_{22} & \bar{Q}_{26} \\ \bar{Q}_{16} & \bar{Q}_{26} & \bar{Q}_{66} \end{bmatrix}^{(k,p)} \begin{Bmatrix} \varepsilon_x \\ \varepsilon_y \\ \gamma_{xy} \end{Bmatrix} \tag{1}$$

where $\bar{Q}_{ij}^{(k,p)}$ (i, j = 1, 2, 6) are converted constants from the stiffness coefficients in the material coordinates

$$Q_{11} = E_L / \left(1-\nu_{LT}\nu_{TL}\right), Q_{22} = E_T / \left(1-\nu_{LT}\nu_{TL}\right), Q_{12} = \nu_{TL}Q_{11} = \nu_{LT}Q_{22}, Q_{66} = G_{LT} \tag{2}$$

(subscript *k* and *p* are dropped for simplicity), by considering $\theta_{k,p}$ around *z*-axis [1, 2].

The potential energy is expressed as

$$U = \sum_{p=1}^{P} \frac{1}{2} \iint_A \{\kappa\}^T \left[D_p\right] \{\kappa\} \, dA_p \tag{3}$$

and the kinetic energy due to vibration is

$$T = \frac{1}{2} \rho h \iint_A \left(\frac{\partial W}{\partial t} \right)^2 dA \tag{4}$$

In Eq.(3), the curvature vector $\{\kappa\}$ is expressed in

$$\{\kappa\} = \left\{ -\frac{\partial^2 W}{\partial x^2} \quad -\frac{\partial^2 W}{\partial y^2} \quad -2\frac{\partial^2 W}{\partial x \partial y} \right\}^T \tag{5}$$

Each element in the bending stiffness matrix $[D_p]$ is given in a subdivision p by

$$D_{ij} = \frac{1}{3} \sum_{k=1}^{K} \bar{Q}_{ij}^{(k,p)} \left(z_k^3 - z_{k-1}^3 \right) \qquad (i, j = 1, 2, 6) \tag{6}$$

The dimensionless coordinates ξ, η are introduced to simplify the analysis. The out-of-plane displacement (deflection) is written as

$$W(\xi, \eta, t) = \sum_{m=0}^{M-1} \sum_{n=0}^{N-1} A_{mn} X_m(\xi) Y_n(\eta) \exp(i\omega t) \tag{7}$$

where

$$X_m(\xi) = \xi^m (\xi + 1)^{bc1} (\xi - 1)^{bc3}, \quad Y_n(\eta) = \eta^n (\eta + 1)^{bc2} (\eta - 1)^{bc4} \tag{8}$$

In Eq.(8), $X_m(\xi)$ and $Y_n(\eta)$ are formulated to meet the kinematical boundary conditions automatically. The bci (i=1, 2, 3, 4) is the boundary condition index, and is set here as $bc1=2$, $bc2=bc3=bc4=0$ for cantilever edge condition in Fig. 1.

The eigenvalue equation for Ω is derived by applying the minimizing process

$$\frac{\partial}{\partial A_{mn}} \left(T_{\max} - U_{\max} \right) = 0 \tag{9}$$

(m=0,1,2,..,M-1; n= 0,1,2,…,N-1) that yields

$$\sum_{m=0}^{M-1} \sum_{n=0}^{N-1} \left(\left[K\right] - \Omega^2 \left[M\right] \right) \left\{A_{mn}\right\} = 0 \tag{10}$$

where $[K]$ and $[M]$ are the stiffness and mass matrix, respectively, in the global coordinates. In the case of the laminate composed of P subdivisions A_1, A_2, ..., A_P, $[K]$ is given by

$$\left[K\right] = \sum_{p=1}^{P} \left[K_p\right] \tag{11}$$

where $[K_p]$ represents the individual stiffness influence stemming from p-th subdivision A_p as

$$K_p = d_{11} f_p^{2200} + \alpha^2 d_{12}\left(f_p^{2002} + f_p^{0220}\right) + \alpha^4 d_{22} f_p^{0022} + 2\alpha d_{16}\left(f_p^{2101} + f_p^{1210}\right) + 2\alpha^3 d_{26}\left(f_p^{0121} + f_p^{1012}\right) + 4\alpha^2 d_{66} f_p^{1111} \tag{12}$$

With

$$f_p^{k\bar{k}l\bar{l}} = \left(\int_{\xi_{p-1}}^{\xi_p} \frac{d^{(k)}X_m(\xi)}{d\xi^{(k)}} \frac{d^{(\bar{k})}X_{\bar{m}}(\xi)}{d\xi^{(\bar{k})}} d\xi\right) \times \left(\int_{-1}^{1} \frac{d^{(l)}Y_n(\eta)}{d\eta^{(l)}} \frac{d^{(\bar{l})}Y_{\bar{n}}(\eta)}{d\eta^{(\bar{l})}} d\eta\right) \tag{13}$$

3. Numerical results and discussions

Numerical results are given by using elastic material constants

E_L = 150.0 GPa, E_T = 10.0 GPa, G_{LT} = 5.0 GPa, ν_{LT} = 0.3. (14)

These constants represent the averaged characteristics for a commercial prepreg sheet of carbon fiber reinforced plastics (so-called, CFRP), and use of these quantities was validated in [24] where approximate frequency formulas are derived by linear regression analysis and results are validated by testing accuracy of the formulas.

It is logical to place blended layers in the outer-most layers on or near the surface, since the bending stiffness is proportional to cubic polynomial in the thickness coordinates. In the present result, symmetric twelve-layer plates are used as examples. The stacking sequence of twelve layers is expressed as

$$\left[\left(\theta_1^{A1} / \theta_1^{A2}\right) / \left(\theta_2^{A1} / \theta_2^{A2}\right) / \underline{0^\circ / 45^\circ / 90^\circ / -45^\circ}\right]_S \tag{15}$$

To have two common subdivisions A_1 and A_2 in the two outer layers of the half thickness. Numbers in the bracket denote the fiber orientation angles from x axis, and a symbol "°" of degree is removed hereafter. Thus, outer two layers include variable fiber angles. Symmetric eight layers [0/45/90/-45]s adjacent to the middle surface constitute the inner base layers that reveal quasi-isotropy, where isotropy can be assumed in stretching within the plane but not in bending.

Table 1 presents convergence study of the present method for rectangular plates (a/b=2). In all cases, the lowest six frequency parameters converge rapidly with increase of series terms from 4×4 (For less number of terms than 4×4, it was not possible to calculate numerically for eigenvalues) to 12×12. The first case is a simply supported, specially orthotropic rectangular plate made of a single layer with fiber angle [0], where the exact solution is available in double sinusoidal function form and is used as a benchmark test of the solution. It is seen that the frequency values from 8×8 solution agree with the exact solution with four significant figures.

The next wo examples deal with cantilever laminated plates with blended layers, where twelve layers [($15^{A1}/30^{A2}$)/ ($15^{A1}/30^{A2}$)/0/45/90/-45]s and [($15^{A1}/30^{A2}$)/ ($-15^{A1}/-30^{A2}$)/0/45/90/-45]s are considered, and the boundary position between two subdivisions as c_1/a = 0.6. The difference between two examples is that the first case is to have unidirectional angles and the second one is to have alternating angle-ply sequence in the outer two blended layers. Comparison is made also with the finite element code developed by [23], and excellent agreement is also shown by the percentage difference with the 12×12 Ritz solution, less than one percent. When a pair of six frequencies are compared between two examples, those in the latter (angle-ply blended layers) give higher frequency values than the former (unidirectional blended layer).

Table 1: Convergence of the present Ritz method for simply supported plate with no blended layer and for two types of cantilever plates with blended layers (a/b=2)

			Ω_1	Ω_2	Ω_3	Ω_4	Ω_5	Ω_6
$[0]_s$	(simple supported plate with no blended layer)							
	Ritz	4×4	63.48	170.8	175.1	254.7	-	-
		6×6	63.47	170.2	174.4	253.9	364.8	375.7
		8×8	63.47	170.2	174.4	253.9	359.2	369.9
		10×10	63.47	170.2	174.4	253.9	359.2	369.8
	Exact solution		63.47	170.2	174.4	253.9	359.2	369.8
$[(15^{A1}/30^{A2})/(15^{A1}/30^{A2})/0/45/-45/90/-45]_s$ (cantilever plate with blended layers)								
	Ritz	4×4	10.96	30.18	67.54	103.8	-	-
		6×6	10.94	30.04	67.16	100.6	144.2	184.7
		8×8	10.93	30.01	66.99	100.4	143.0	183.3
		10×10	10.92	30.00	66.91	100.3	143.0	183.2
		12×12	10.92	29.99	66.86	100.3	142.9	183.1
	FEM	10×10	10.91	29.96	66.84	100.1	142.7	182.1
	dif. (%)		0.09	0.10	0.03	0.19	0.17	0.57
$[(15^{A1}/30^{A2})/(-15^{A1}/-30^{A2})/0/45/-45/90/-45]_s$ (cantilever plate with blended layers)								
	Ritz	4×4	12.13	34.56	71.59	131.3	-	-
		6×6	12.09	34.44	71.33	128.7	145.8	201.5
		8×8	12.09	34.42	71.22	128.5	144.8	200.7
		10×10	12.08	34.41	71.15	128.4	144.8	200.6
		12×12	12.09	34.41	71.12	128.4	144.8	200.5
	FEM	10×10	12.08	34.41	71.11	128.4	144.6	201.3
	dif. (%)		0.08	0.00	0.01	0.01	0.12	-0.40

Table 2 lists frequency parameters of the plates with $[(\theta^{A1}/\theta^{A2})/ (\theta^{A1}/\theta^{A2})/\underline{0/45/90/-45}]$s, where two outer layers are unidirectional to have the same angles. Values of θ^{A1} and θ^{A2} are taken as 0°, 15°, 30° and 45°. The angle difference between θ^{A1} and θ^{A2} is kept less or equal to 45°, because it is a common practice to avoid sharp kink of fibers along the boundary of two adjacent subdivisions.

Table 3 is the same format as Table 2, but the two blended layers are alternating angle-ply sequence as $[(\theta^{A1}/\theta^{A2})/ (-\theta^{A1}/-\theta^{A2})/\underline{0/45/90/-45}]$s. It is observed by the comparison with Table 2 that these frequency parameters are generally higher than those in Table 2, and from design viewpoint it is recommended to have angle-ply sequence in the outer two blended layers to increase the natural frequencies.

Table 2: Frequency parameters Ω of cantilevered 12-layered plates with various fiber orientations in unidirectional blended layers $[(\theta_1^{A1}/\theta_1^{A2})/(\theta_2^{A1}/\theta_2^{A2})/0/45/90/-45]$S, ($a/b$=2, c_1/a=0.6).

θ_1^{A1}	θ_1^{A2}	θ_2^{A1}	θ_2^{A2}	Ω_1	Ω_2	Ω_3	Ω_4	Ω_5	Ω_6
0	0	0	0	12.91	26.94	80.76	103.6	129.6	195.2
0	15	0	15	12.85	27.32	77.14	104.1	131.1	190.6
0	30	0	30	12.76	28.44	71.12	106.1	139.6	193.0
0	45	0	45	12.69	28.68	66.45	104.0	156.5	192.5
15	0	15	0	11.14	28.51	75.27	96.87	134.0	192.1
15	15	15	15	11.01	28.92	71.91	98.00	135.9	183.6
15	30	15	30	10.92	30.00	66.91	100.3	143.0	183.2
15	45	15	45	10.91	30.20	62.97	98.21	155.2	183.1
30	0	30	0	8.880	30.73	63.44	91.93	138.8	190.8
30	15	30	15	8.800	30.94	61.38	92.60	140.8	177.9
30	30	30	30	8.740	31.88	57.78	95.66	143.9	173.9
30	45	30	45	8.720	32.09	54.89	94.77	145.1	174.7
45	0	45	0	7.540	29.92	52.95	89.06	141.7	173.1
45	15	45	15	7.510	30.05	51.72	89.19	142.2	171.3
45	30	45	30	7.470	30.79	49.25	92.48	139.0	168.5
45	45	45	45	7.450	30.89	47.17	92.73	132.5	169.8

Table 3: Frequency parameters Ω of cantilevered 12-layered plates with various fiber orientations in angle-ply blended layers [($\theta_1^{A1}/\theta_1^{A2}$)/($\theta_2^{A1}/\theta_2^{A2}$)/0/45/90/-45]S, ($a/b$=2, c_1/a=0.6).

θ_1^{A1}	θ_1^{A2}	θ_2^{A1}	θ_2^{A2}	Ω_1	Ω_2	Ω_3	Ω_4	Ω_5	Ω_6
0	0	0	0	12.91	26.94	80.76	103.6	129.6	195.2
0	15	0	-15	12.89	28.95	79.24	112.9	131.7	211.0
0	30	0	-30	12.83	30.89	74.21	127.5	140.3	205.8
0	45	0	-45	12.73	31.23	67.82	135.6	156.0	194.8
15	0	-15	0	12.17	30.26	77.14	103.9	133.6	202.9
15	15	-15	-15	12.15	32.35	75.73	113.3	136.3	213.2
15	30	-15	-30	12.08	34.41	71.15	128.4	144.8	200.6
15	45	-15	-45	12.00	34.84	65.41	136.1	158.3	192.9
30	0	-30	0	10.28	35.42	67.19	104.5	140.9	201.4
30	15	-30	-15	10.27	37.73	66.13	114.0	145.0	197.3
30	30	-30	-30	10.21	10.09	62.72	129.9	153.0	187.3
30	45	-30	-45	10.15	40.68	58.52	137.0	155.0	193.9
45	0	-45	0	8.250	37.15	55.80	101.9	146.5	178.8
45	15	-45	-15	8.240	39.52	55.12	111.5	152.0	176.1
45	30	-45	-30	8.200	41.92	52.89	127.5	152.8	178.6
45	45	-45	-45	8.170	42.55	50.10	133.9	142.3	201.5

Figures 2(a) and (b) present variations of frequency parameters against location of subdivision boundary C_1=2x/a for cantilevered, symmetrically laminated twelve-layer plates with laminate sequence (a) [($0^{A1}/45^{A2}$)/ (0^{A1}/-45^{A2})/0/45/90/-45]s and (b) [(15^{A1}/-30^{A2})/ (-15^{A1}/30^{A2})/0/45/90/-45]s, respectively. In both cases, the first and third frequencies Ω_1 and Ω_3 increase as the subdivision boundary moves from clamped edge (2x/a= -1) to the free end (2x/a=1), while other three frequencies Ω_2,Ω_4 and Ω_5 decrease. These observations suggest that the location of subdivision boundary can be used in the optimum design in addition to the fiber orientation angles.

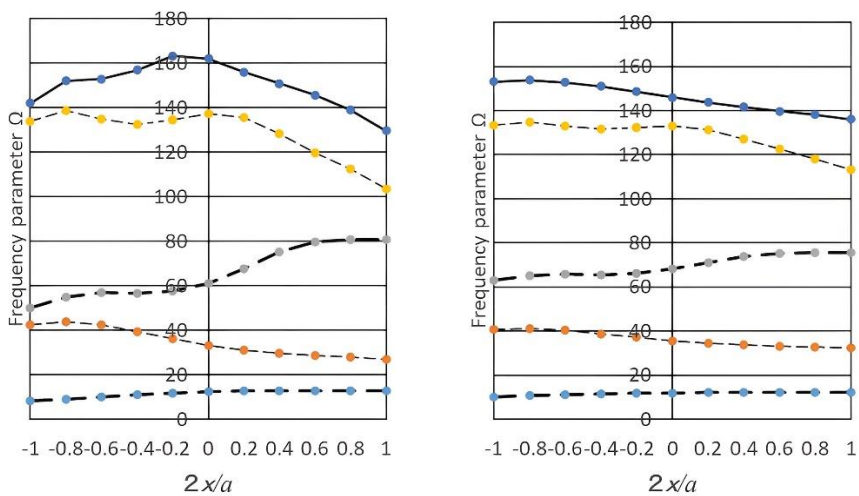

(a) [($0^{A1}/45^{A2}$)/ (0^{A1}/-45^{A2})/0/45/90/-45]s (b) [(15^{A1}/-30^{A2})/ (-15^{A1}/30^{A2})/0/45/90/-45]s

Fig. 2. Variations of frequency parameters Ω vs. location c_1/a of boundary between subareas.

Figure 3 presents the mode shapes of the plate used in the first example of Table 1. A circle in the figures indicates location of the maximum amplitude. In the 1st mode (first bending mode), the maximum amplitude at one corner point is greater than the other corner point about 38 percent, and contour lines are skewed by the fiber angles. Similarly in the 2nd mode (first twisting mode) the maximum amplitude is greater about ten percent, and a nodal line (i.e., line of zero deflection) is skewed significantly deviating from a line of symmetry perpendicular to the clamped edge. As observed also in 3rd and 4th modes, the nodal lines and contours are considerably affected by the presence of blended layers. The present mode shapes appear exactly same as those calculated by the self-made FEM and no difference is observed in the figures, although the frequency values are slightly different as listed in Table 1.

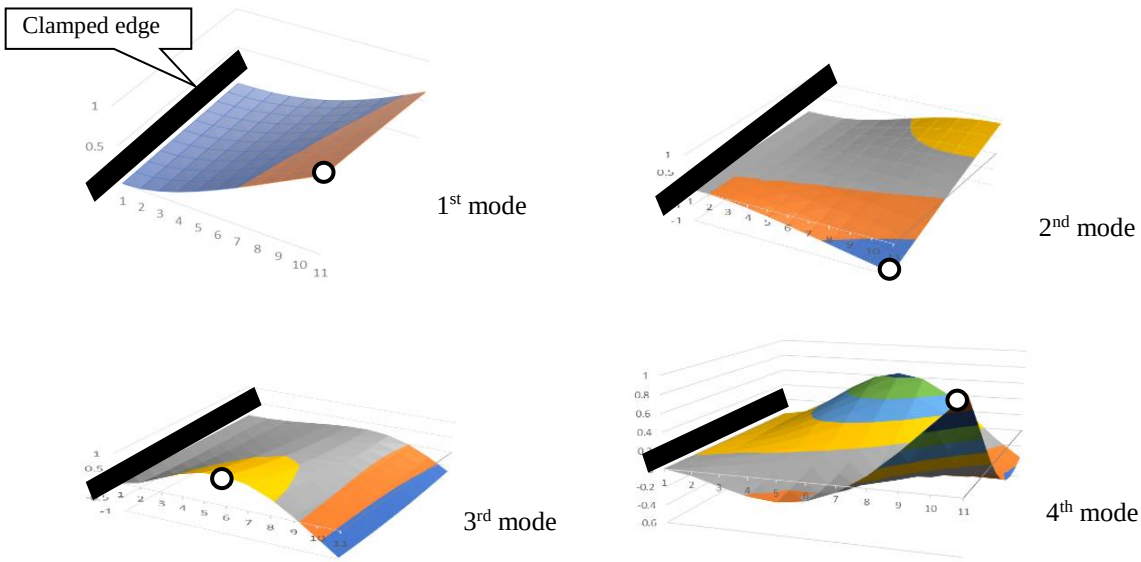

Fig. 3. Mode shapes of plates used as the first example in Table 1 (○: maximum amplitude).

4. Conclusions

An approach was proposed to study the free bending vibration of a cantilevered, laminated rectangular plate having a few subdivisions with non-identical fiber orientations. These so-called blended layers with subdivisions of different nature were taken in account. Convergence tendency was confirmed and comparison with the finite element code developed by the author showed excellent agreement. In numerical study, two types of blended layers are tested for the cantilevered twelve-layered plates. It is found that angle-ply sequence in the blended layers is advantageous to increase the natural frequencies, and use of blended layers is recommended under reasonable cost to widen the possibility of composites with straight fiber.

Acknowledgement

This work was supported by JSPS KAKENHI Grant Number JP21K03957.

Nomenclature

A	area of a plate
A_{mn}	undetermined coefficient in assumed amplitude
A_p	area of p-th subdivision
a	length of plate edge in x direction
b	length of plate edge in y direction
bc	boundary index
D_{ij}	bending stiffness (i,j=1,2,6)
D_0	reference stiffness, $D_0 = E_T h^3 / 12(1-\nu_{LT}\nu_{TL})$
D_p	bending stiffness in the p-th subdivision
d_{ij}	dimensionless stiffness, $d_{ij} = D_{ij} / D_0$
E_L	Young's modulus in fiber direction
E_T	Young's modulus in the direction perpendicular to fiber
G_{LT}	shear modulus in LT plane
h	thickness of plate
K	number of layers in laminated plate
L	fiber direction in lamina

M	upper limit in series terms in *x* direction
m	number of series terms in *x* direction
N	upper limit in series terms in *y* direction
n	number of series terms in *y* direction
$\bar{Q}_{ij}^{(k,p)}$	material constants in *x*,*y* coordinates converted from the stiffness coefficients (*i*, *j* = 1, 2, 6)
$Q_{ij}^{(k,p)}$	material constants in *L*,*T* coordinates in the material coordinates (*i*, *j* = 1, 2, 6)
T	kinetic energy
U	potential energy
W	deflection of plate
$X_m(\xi)$	assumed displacement function in *x* direction
$Y_n(\eta)$	assumed displacement function in *y* direction
x,*y*	coordinates
z	thickness coordinate from middle surface
α	aspect ratio, $\alpha = a/b$
η	dimensionless coordinate, $\eta = 2y/b$
$\theta_{k,p}$	fiber orientation angle in *p*-th subarea measured from x axis around *z*-axis
ν_{LT}, ν_{TL}	major and minor Poison's ratio
ξ	dimensionless coordinate, $\xi = 2x/a$
ρ	averaged density, kg/m^3
Ω	dimensionless frequency parameter, $\Omega = \omega a^2(\rho h/D_0)^{1/2}$

Subscripts

p	*p*-th subdivision

References

[1] Vinson JR, Sierakowski RL. The behavior of structures composed of composite materials. Dordrecht: Kluwer Academic; 1986.

[2] Jones RM. Mechanics of composite materials. 2nd ed. Boca Raton: CRC Press; 1999.

[3] Leissa AW, Qatu MS. Vibration of continuous systems. New York: McGraw-Hill; 2021.

[4] Dutton S, Kelly D, Baker A. Composite materials for aircraft structures. 2nd ed. Reston: AIAA Education; 2004.

[5] Harris CE, Starnes JH, Shuart MJ. Design and manufacturing of aerospace composite structures, state-of-the-art assessment. J Aircr. 2002;39(4):545-560.

[6] Panesar AS, Weaver PM. Optimisation of blended bistable laminates for a morphing flap. Compos Struct. 2012;94(10):3092-3105.

[7] Leissa AW. Vibration of plates NASA SP-160. Washington: U.S. Government Printing Office; 1969. Republished from: The Acoustical Society of America; 1993.

[8] Leissa AW, Macbain JC, Keilb RE. Vibrations of twisted cantilevered plates—summary of previous and current studies. J Sound Vib. 1984;96(2):159-173.

[9] Narita Y, Leissa AW. Frequencies and mode shapes of cantilevered laminated composite plates. J Sound Vib. 1992;154(1):161-172.

[10] Ghiasi H, Pasini D, Lessard L. Optimum stacking sequence design of composite materials Part I: constant stiffness design. Compos Struct. 2009;90(1):1-11.

[11] Ghiasi H, Fayazbakhsh K, Pasini D, Lessard L. Optimum stacking sequence design of composite materials Part II: variable stiffness design. Compos Struct. 2010;93(1):1-13.

[12] Abdalla MM, Setoodeh S, Gürdal Z. Design of variable stiffness composite panels for maximum fundamental frequency using lamination parameters. Compos Struct. 2007;81(2):283-291.

[13] Akhavan H, Ribeiro P. Natural modes of vibration of variable stiffness composite laminates with curvilinear fibers. Compos Struct. 2011;93(11):3040-3047.

[14] Ribeiro P, Akhavan H, Teter A, Warmiński J. A review on the mechanical behaviour of curvilinear fibre composite laminated panels. J Compos Mater. 2014;48(22):2761-2777.

[15] Honda S, Oonishi Y, Narita Y, Sasaki K. Vibration analysis of composite rectangular plates reinforced along curved lines. J Syst Des Dyn. 2008;2(1):76-86.

[16] Honda S, Narita Y. Design for the maximum natural frequency of laminated composite plates by optimally distributed short fibers. J Syst Des Dyn. 2008;2(6):1195-1205.
[17] Honda S, Narita Y, Sasaki K. Maximizing the fundamental frequency of laminated composite plates with optimally shaped curvilinear fibers. J Syst Des Dyn. 2009;3(6):867-876.
[18] Honda S, Narita Y. Vibration design of laminated fibrous composite plates with local anisotropy induced by short fibers and curvilinear fibers. Compos Struct. 2011;93(2):902-910.
[19] Honda S, Narita Y. Natural frequencies and vibration modes of laminated composite plates reinforced with arbitrary curvilinear fiber shape paths. J Sound Vib. 2012;331(1):180-191.
[20] Honda S, Takisawa H, Takeda R, Sasaki K, Katagiri K. Estimation of damping characteristics and optimization of curvilinear fiber shapes for composites fabricated by electrodeposition resin molding. Mech Adv Mater Struct. 2023;30(21):4407-4418.
[21] Zein S, Bruyneel M. A bilevel integer programming method for blended composite structures. Adv Eng Softw. 2015;79:1-12.
[22] Muc A. Design of blended/tapered multilayered structures subjected to buckling constraints. Compos Struct. 2018;186:256-266.
[23] Innami M, Honda S, Sasaki K, Narita Y. Analysis and optimization for vibration of laminated rectangular plates with blended layers. Compos Struct. 2021;274:114400.
[24] Narita Y, Innami M, Narita D. The effect of using different elastic moduli on vibration of laminated CFRP rectangular plates. EPI Int J Eng. 2019;2(1):19-27.